Supplementary Information (SI) for Energy & Environmental Science.
This journal is © The Royal Society of Chemistry 2024

Supplementary Information

Interfacial degradation of silicon anode in pouch cells

Qiu Fang[1,2], Shiwei Xu[1,3], Xuechao Sha[4], Di Liu[4], Xiao Zhang[1,2], Weiping Li[1,2], Suting Weng[1,3], Xiaoyun Li[1,2], Liquan Chen[1], Hong Li[1,2,3,7], Bo Wang[5,6]*, Zhaoxiang Wang[1,2,3]* and Xuefeng Wang[1,2,3]*

[1]Beijing National Laboratory for Condensed Matter Physics, Institute of Physics, Chinese Academy of Sciences, Beijing 100190, China

[2]College of Materials Science and Opto-Electronic Technology, University of Chinese Academy of Sciences, Beijing 100049, China

[3]School of Physical Sciences, University of Chinese Academy of Sciences, Beijing 100049, China

[4]ZEISS Research Microscopy Solutions, Carl Zeiss (Shanghai) Co. Ltd., Shanghai 200131, China

[5]Watt Lab, Central Research Institute, Huawei Technologies Co., Ltd., Shenzhen 518129, China

[6]State Key Laboratory of Space Power-Sources, School of Chemistry and Chemical Engineering, Harbin Institute of Technology, Harbin 150001, China

[7]Tianmu Lake Institute of Advanced Energy Storage Technologies Co. Ltd., Liyang 213300, Jiangsu, China

*Corresponding authors: wxf@iphy.ac.cn (Xuefeng Wang); zxwang@iphy.ac.cn (Zhaoxiang Wang.); wangbo19880804@163.com (Bo Wang).

Experimental section

Preparation of electrodes and cell assembly

Home-made pouch cells for electrochemical test (450 mAh) employed commercial $LiCoO_2$ cathode (three layers, with mass loading of 16.88 mg cm^{-2} and areal capacity of 3.03 mAh cm^{-2}), Si anode (four layers, with mass loading of 2.99 mg cm^{-2} and areal capacity of 3.84 mAh cm^{-2}), and electrolyte. The N/P ratio of pouch cells is 1.27.

CR2032 half-cells used for electrochemical evaluation of $LiCoO_2$ after cycles were assembled in an argon-filled glove box (O_2 < 0.1 ppm and H_2O < 0.1 ppm). $LiCoO_2$ electrode (φ8 mm) extracted from pouch cells was employed as the cathode with lithium foil (φ16.2 mm, 600 μm in thickness) as the anode and Celgard 2400 membrane (φ16.2 mm) as the separator. Commercial electrolyte used in the pouch cells was also employed in the coin cell (120 μL).

Sulfur powder (0.2 mg mL^{-1}) was added to the above electrolyte and dissolved through ultrasonic dispersion for 30 minutes. For Si electrodes, slurry was prepared by dispersing commercial Si microparticles (used in pouch cells), polyacrylic acid binder and acetylene black in water with a weight ratio of 8:1:1. The slurry was cast on copper foil, dried at 55 °C and further dried at 120 °C overnight under vacuum. The prepared Si electrodes (φ10 mm) shows a mass loading of 2.5–3 mg cm^{-2}.

Electrochemical measurements

Pouch cells were tested on a NEWARE battery test system (CT-4008T-5V6A-S1-F) and cycled between 3.00 and 4.42 V (*vs.* Li^+/Li) under 25 °C (±3 °C). Before cycling, pouch cells were activated through constant current charging (CC charging) to 4.42 V at 0.5 C, then constant voltage charging (CV charging) to 11.25 mA (0.025 C) and CC discharging at 0.5 C, finally CV discharging to 11.25 mA (0.025 C). During charging process, the cells were first CC charged to 4.10 V at 1.5 C and CV charged to 337.5 mA (0.75 C), then CC charged to 4.25 V at 0.75 C and CV charged to 225 mA (0.5 C), finally CC charged to 4.42 V at 0.5 C and CV charged to 11.25 mA (0.025 C). During discharging process, the cells were CC discharged to 3.00 V at 0.7 C and CV discharged to 11.25 mA (0.025 C).

The electrochemical performance data of the pouch cell are based on one-time measurement. The capacity retention shown in Fig 1a is calculated through dividing the discharge capacity at the 300^{th} cycles by the discharge capacity at the 1^{st} cycle. The charge capacity and discharge capacity during the activation is 447.75 mAh and 437.71 mAh respectively, yielding a coulombic efficiency of 97.758%.

Coin cells used for electrochemical evaluation of $LiCoO_2$ were cycled with the same condition and steps as pouch cells. Coin cells used for electrochemical evaluation of sulfur-added electrolyte were first discharged at 0.3 C (1 C=1500 mA g^{-1}) from 1.000 V to 0.005 V, then further discharged to 0.005 V at 0.05 C, and charged to 1.000 V at 0.5 C.

EIS test of pouch cells was conducted on an electrochemical workstation (BioLogic SP-200 system) under room temperature in the frequency range from 1 MHz to 100 mHz with an a.c. signal of 10 mV.

Characterization

Si electrodes sample after different cycles were milled through cross-section polisher (Fischione 1061 SEM Mill) under −80 °C and transferred in a sealed holder from glove box to a scanning electron microscope (SEM, HITACHI Regulus 8100) for observation. Polished sample of Si electrode after 300 cycles was transferred to a SEM (ZEISS Sigma 360) and Raman spectra of Si

particle were recorded (532 nm radiation) by a plugged-in detector (WITec RISE).

FTIR spectra were acquired under ATR mode with a diamond crystal on a Bruker ALPHA II instrument in an argon-filled glove box. $LiBF_4$ salt as external standard was dissolved in dimethyl carbonate (DMC) to prepare solution (0.025 mol L^{-1}). Then 0.2 μL of the solution was added on the diamond crystal before measurement. After drying, electrode samples were loaded on the ATR crystal for recording.

The XPS measurement was carried out on a Thermo Scientific ESCALAB 250 Xi instrument with monochromatic 150 W (Al $K\alpha$ line) radiation. Electrode samples were loaded on a sealed holder and transferred from glove box to the vacuum chamber. The peak positions of spectra were calibrated using the C–C bond (284.8 eV) signal as reference.

Cryo-(S)TEM characterizations were carried out using a JEOL JEM-F200 microscope under cryogenic temperatures (−180 °C) at 200 kV. The powder sample for cryo-(S)TEM characterizations was scratched from Si electrode rinsed by DMC and dispersed on Cu grid. Then the grid was loaded on the cryo-TEM holder (Fischione 2550) equipped with a tip retraction device in the glove box and transferred into the JEOL JEM-F200 microscope without air exposure with the help of a sealing sleeve. Liquid nitrogen was added to the cryo-TEM holder and temperature of sample was ensured to stabilize at −180 °C before observation under cryo-(S)TEM. The porosity was estimated through Image J software.

Sample preparation employing cryo-FIB was carried out on ZEISS Crossbeam 550. Electrode after 300 cycles was transferred into FIB-SEM instrument and cross-section lamellae of interlayer was prepared under cryogenic temperatures.

The Young's modulus of the SEI on Si electrode after different cycles was obtained by PeakForce QNM mode (Bruker Multimode 8) with the RTESPA-525 tip in an atomic force microscope.

Supplementary results

Table S1 D50 value calculated by statistics analysis from size distribution of Si particles after different cycles.

Si anodes	pristine	after formation	after 10 cycles	after 100 cycles	after 200 cycles	after 300 cycles
D50 (μm)	3.03	3.23	3.55	3.82	3.92	4.04

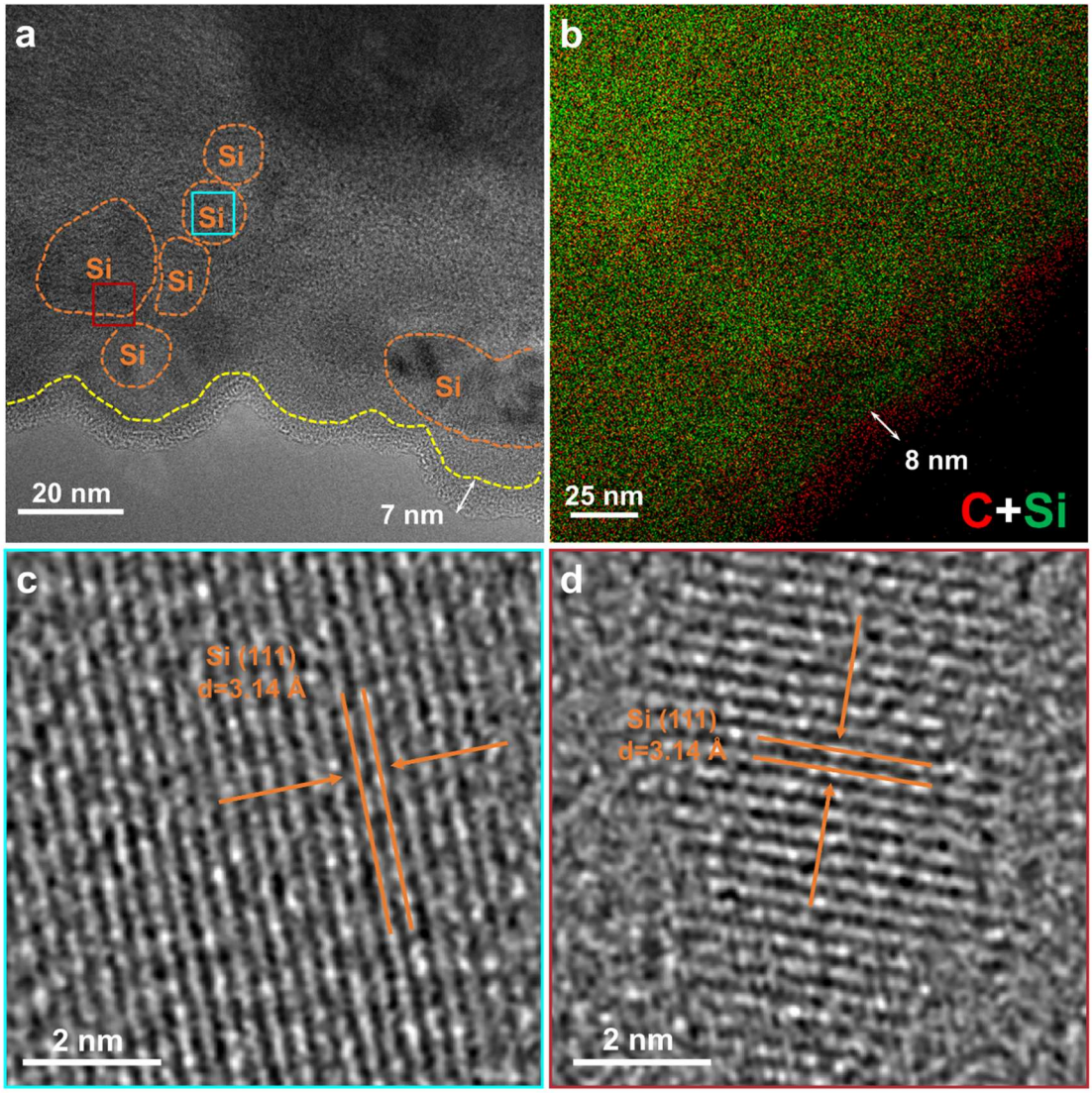

Fig. S1 (a) HRTEM image of the pristine Si particle, (b) elemental mapping of C (in red) and Si (in green) from the pristine Si particle and (c, d) corresponding magnified images of selected areas in (a).

Table S2 Comparison of the initial coulombic efficiency and capacity retention of the pouch cells based on Si anode reported in the literature.

References	Cell composition	Cycle condition	Initial coulombic efficiency	Capacity retention
Our data	**$LiCoO_2$||Si (83 wt% Si) pouch cells (450 mAh) N:P=1.27**	**25±3 °C, 3.0–4.42 V, 1.5 C to 4.1 V, 0.75 C to 4.25 V, 0.5 C to 4.42 V**	**96.43%**	**96.63% after 300 cycles**
Ref[1]	$LiNi_{0.8}Co_{0.15}Al_{0.05}O_2$||Si pouch cells (1.07 Ah), N:P=1.11	20 °C, 2.8–4.1 V, 0.1 C	/	85% after 120 cycles
Ref[2]	$LiNi_{0.5}Co_{0.2}Mn_{0.3}O_2$||Si/graphite (500 mAh g^{-1}) pouch cells (2 Ah), N:P=1.1	room temperature, 2.75–4.2 V, 1 C	/	80.2% after 700 cycles
Ref[3]	$LiNi_{0.5}Co_{0.2}Mn_{0.3}O_2$||Si/graphite (55:45) pouch cells (1861.1 mAh), N:P=1.15	2.75–4.2 V, 1 C	87%	90.1% after 150 cycles
Ref[4]	$LiNi_{0.6}Co_{0.2}Mn_{0.2}O_2$||pre-lithiated Si/graphite (18:70) single layer pouch cells (53.6 mAh), N:P=1.07	25 °C, 2.0–4.4 V, 0.7 C charging, 0.5 C discharging	/	87% after 300 cycles
Ref[5]	$LiCoO_2$||BMSi@GC pouch cells (537 Wh kg^{-1}), N:P=1.1	25 °C, 2.5–4.5 V, 1 A g^{-1}	89.2%	81.9% after 200 cycles
Ref[6]	$LiNi_{0.8}Co_{0.1}Mn_{0.1}O_2$||pre-lithiated Si@C pouch cells (2 Ah), N:P=1.05	room temperature, 2.75–4.2 V, 0.5 C	87.5%	83.8% after 1000 cycles
Ref[7]	$LiNi_{0.95}Co_{0.02}Mn_{0.03}O_2$||Si@G/CNF@NC pouch cells (2 Ah), N:P=1.1	2.8–4.3 V, 0.3 C	/	80% after 80 cycles
Ref[8]	$LiNi_{0.6}Co_{0.2}Mn_{0.2}O_2$|| pre-lithiated PCC-nSi coin cells (CR2025), N:P=1–1.1	3–4.3 V, 1 C (1 C=180 mA g^{-1})	90.4%	80% after 200 cycles
Ref[9]	$Li(Ni_{1/3}Co_{1/3}Mn_{1/3})O_2$|| pre-lithiated AMPSi@C coin cells (CR2016), N:P=1.1	2.8–4.25 V, 0.5 C (1 C=160 mA g^{-1})	94%	80.8% after 120 cycles

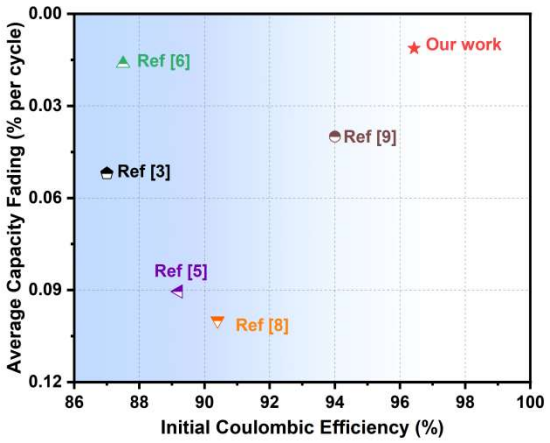

Fig. S2 Comparison of the initial coulombic efficiency and capacity retention of the pouch cells based on Si anode reported in the literature[3, 5, 6, 8, 9].

Table S3 Different resistances calculated by DRT analysis of EIS in Fig. 1d.

Si anode	after 10 cycles	after 100 cycles	after 200 cycles	after 300 cycles
Li^+ transporting through SEI	0.041	0.049	0.055	0.066
anode charge transfer	0.087/0.039	0.072/0.059	0.072/0.048	0.078/0.086
cathode charge transfer	0.146	0.162	0.168	0.187

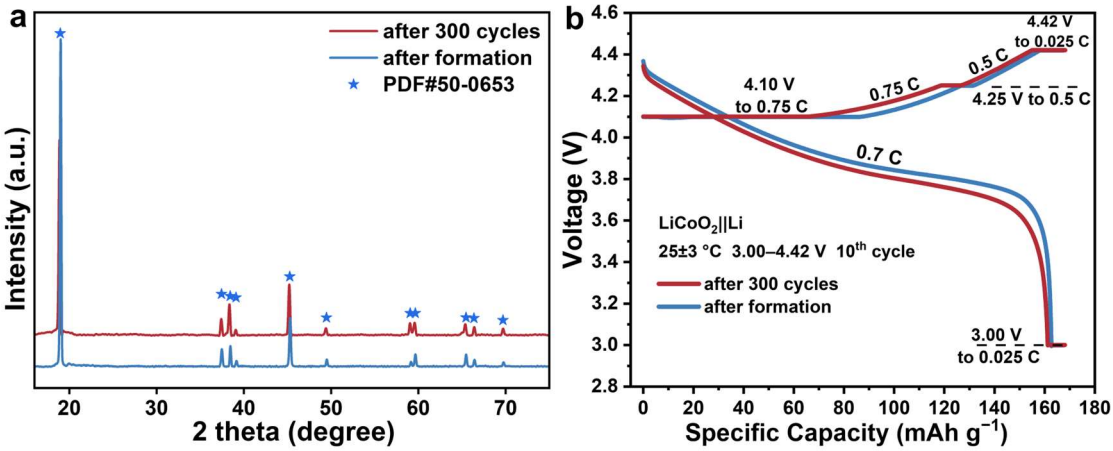

Fig. S3 (a) XRD patterns and (b) voltage profile of the $LiCoO_2$ electrode harvested after formation and 300 cycles.

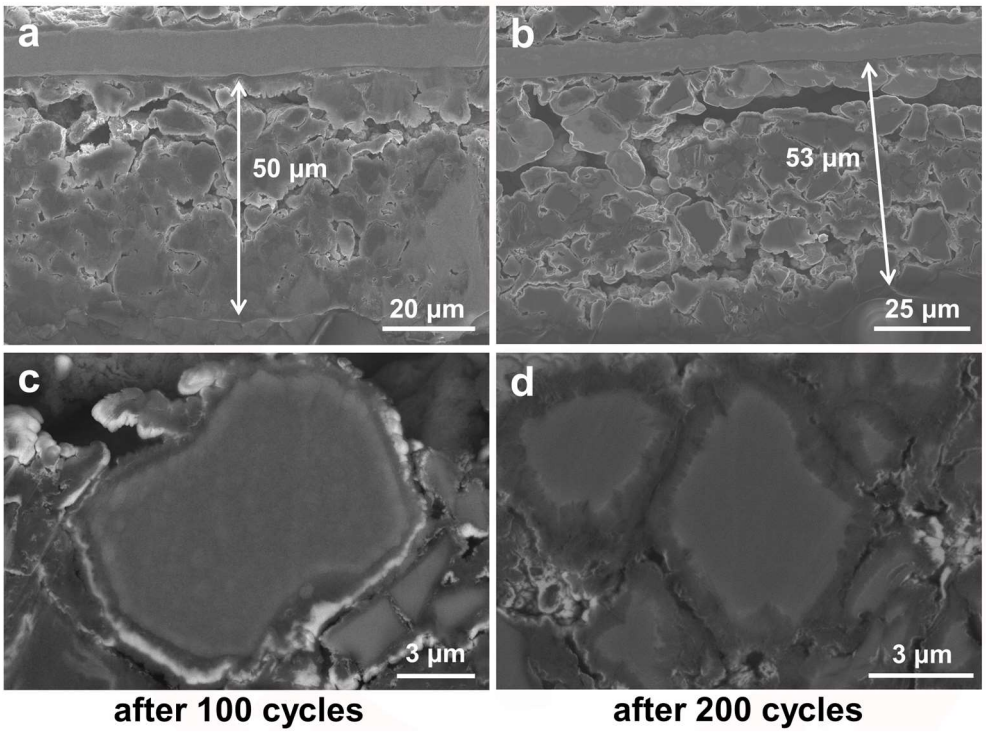

Fig. S4 (a, b) Cross-sectional images and (c, d) magnified images of Si electrodes (a, c) after 100 cycles and (b, d) after 200 cycles.

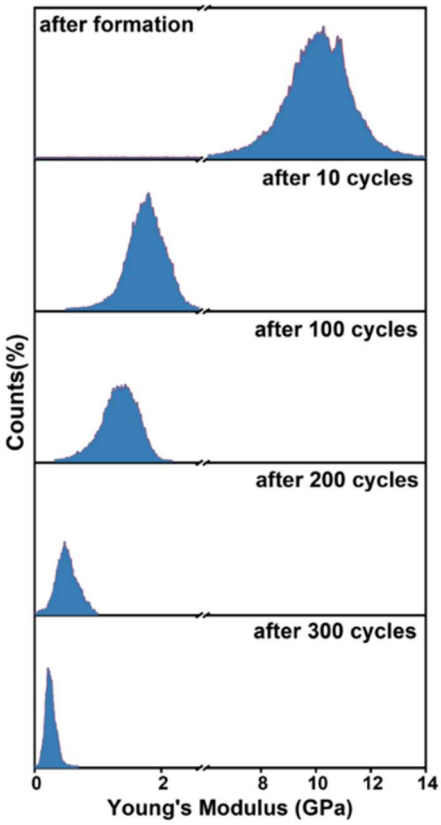

Fig. S5 Young's modulus distribution of Si particles after different cycles measured by atomic force microscopy (AFM). Decreasing Young's modulus indicates reduced mechanical strength of SEI on Si particles during cycles.

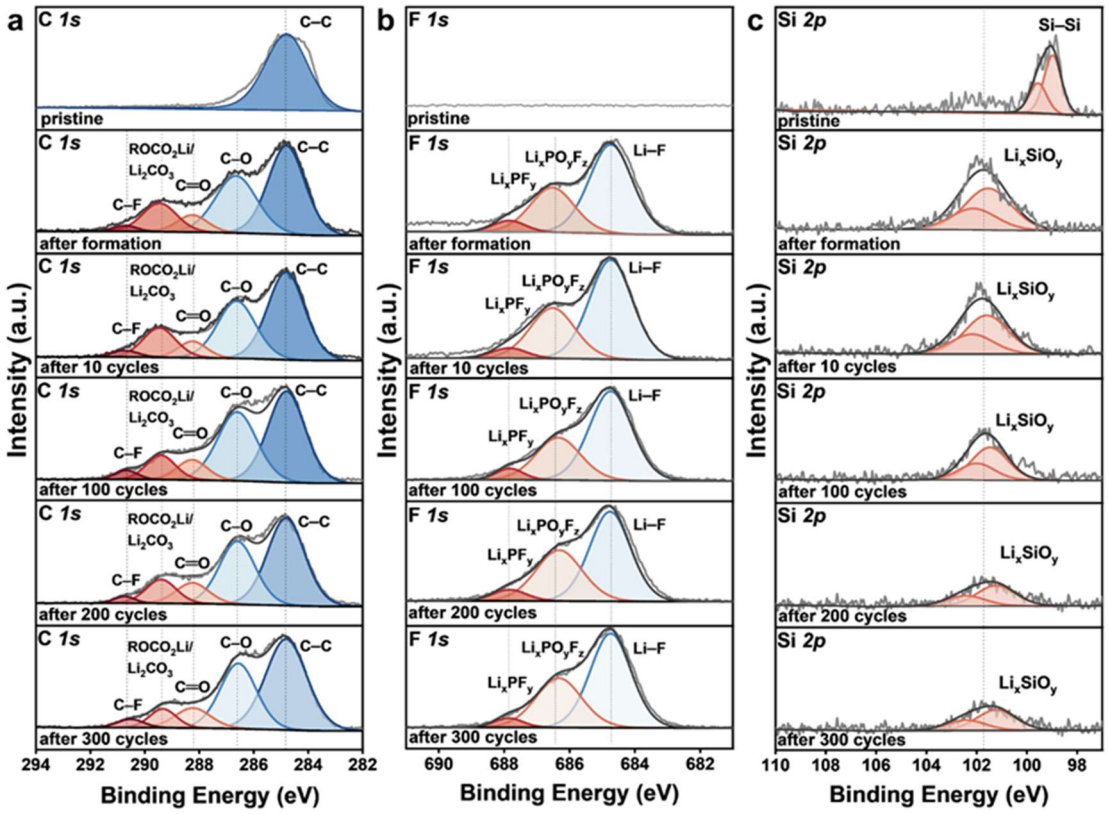

Fig. S6 (a) C *1s*, (b) F *1s*, (c) Si *2p* spectra of the pristine Si electrode, electrodes after formation, after 10, 100, 200, 300 cycles.

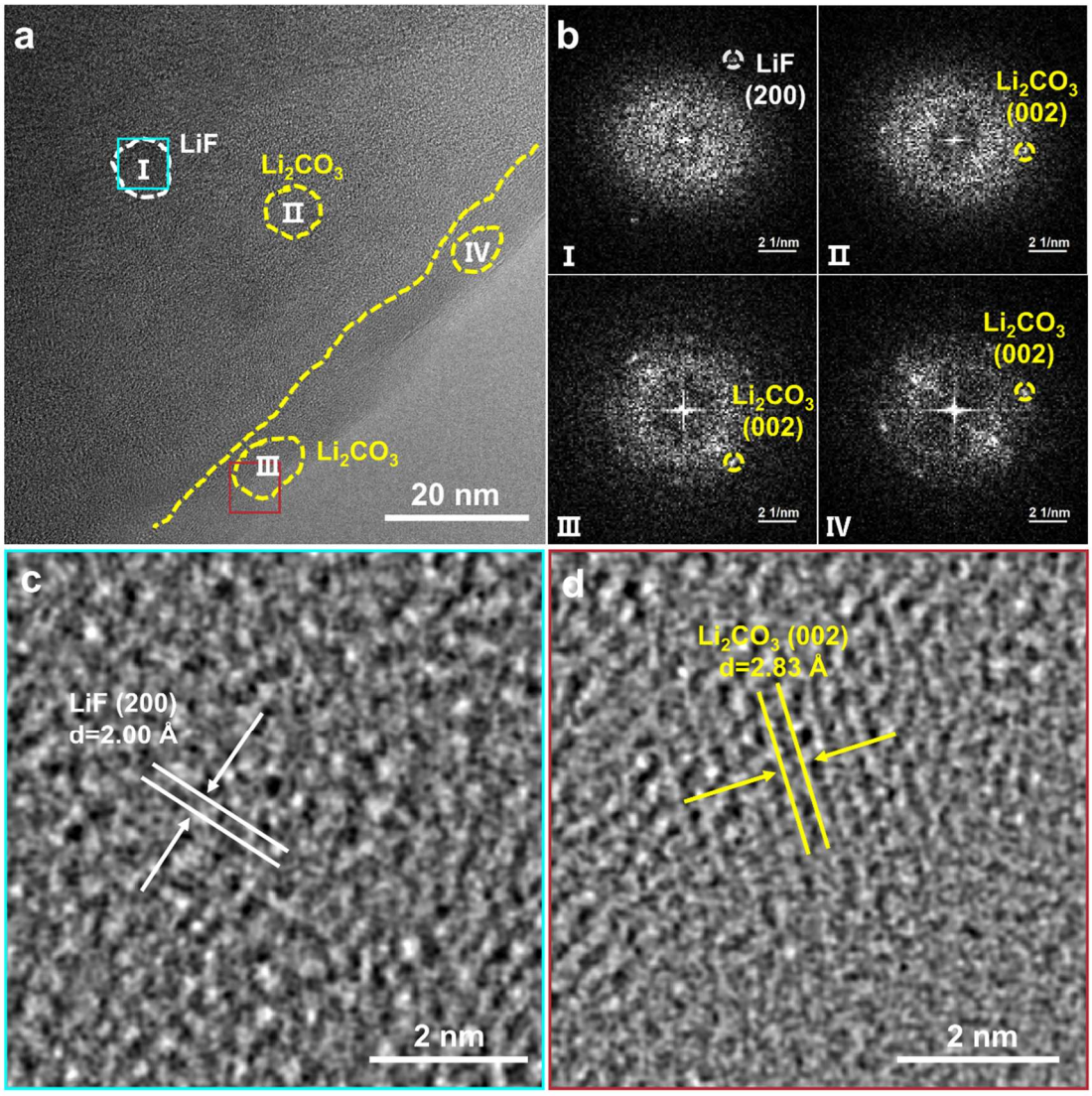

Fig. S7 (a) HRTEM image of Fig. 4a, (b) corresponding fast Fourier transformed images of the Si particle after formation and (c, d) corresponding magnified images of selected areas in (a).

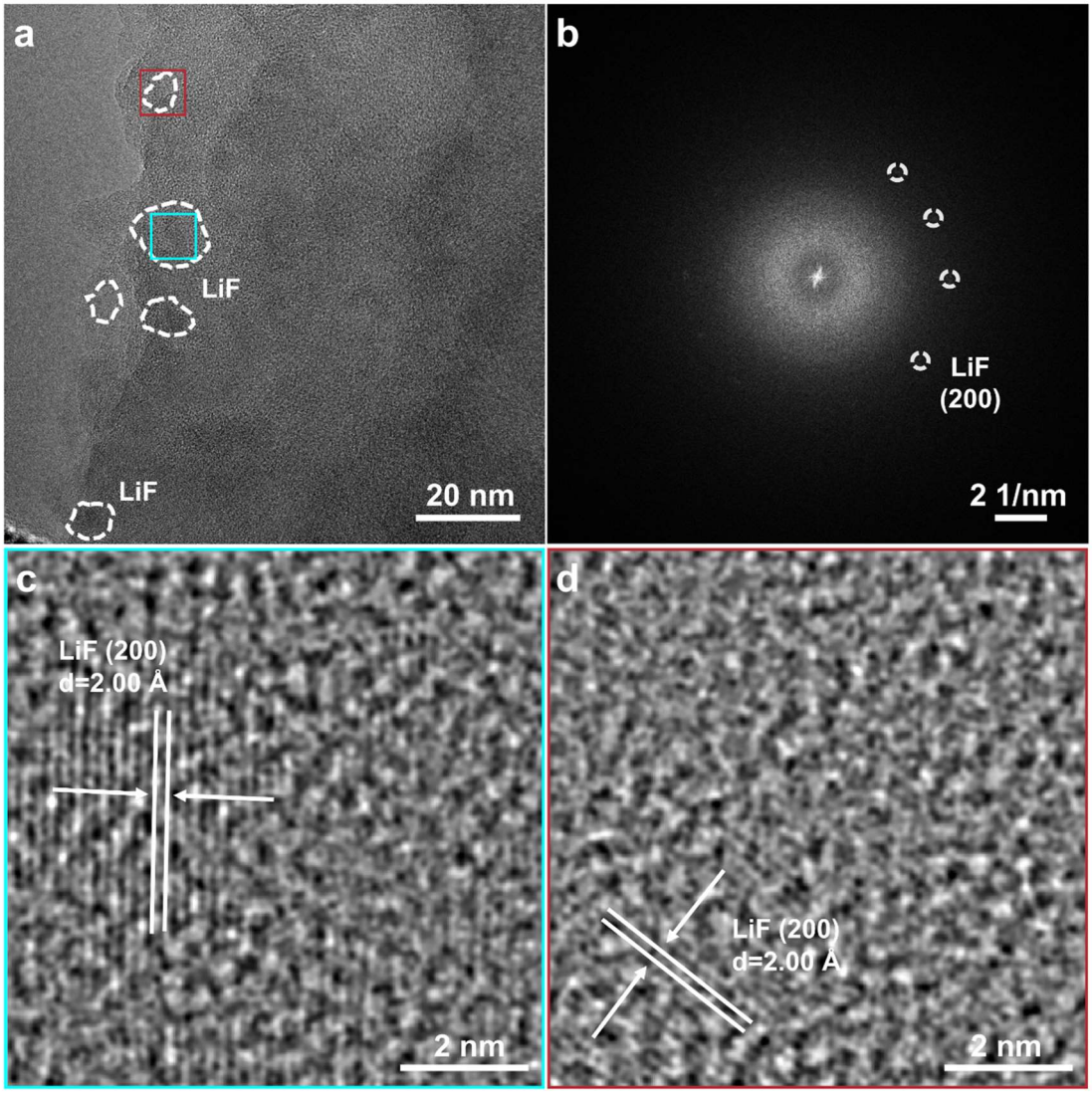

Fig. S8 (a) HRTEM image of Fig. 4b, (b) corresponding fast Fourier transformed images of the Si particle after 10 cycles and (c, d) corresponding magnified images of selected areas in (a).

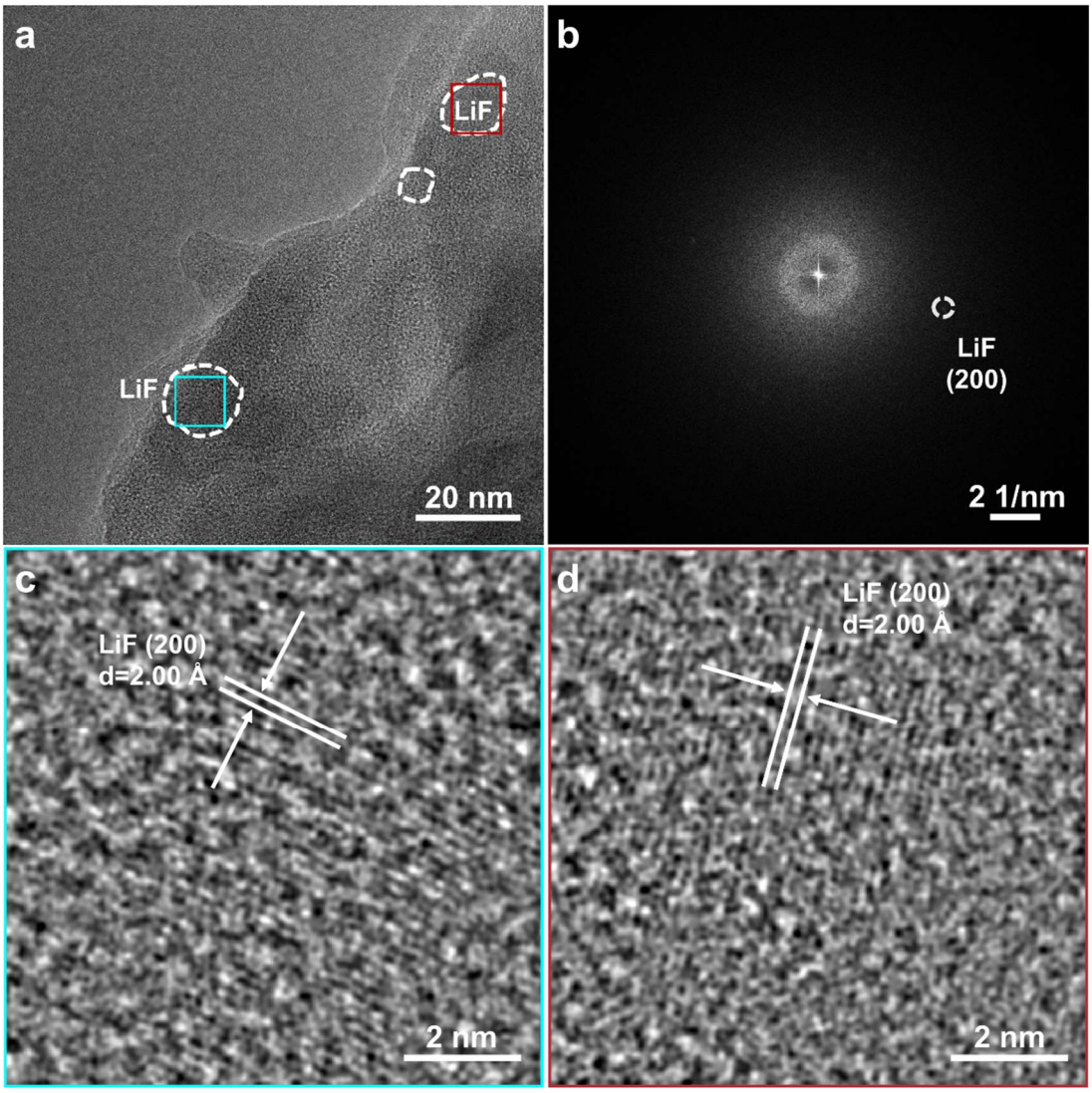

Fig. S9 (a) HRTEM image of Fig. 4c, (b) corresponding fast Fourier transformed images of the Si particle after 100 cycles and (c, d) corresponding magnified images of selected areas in (a).

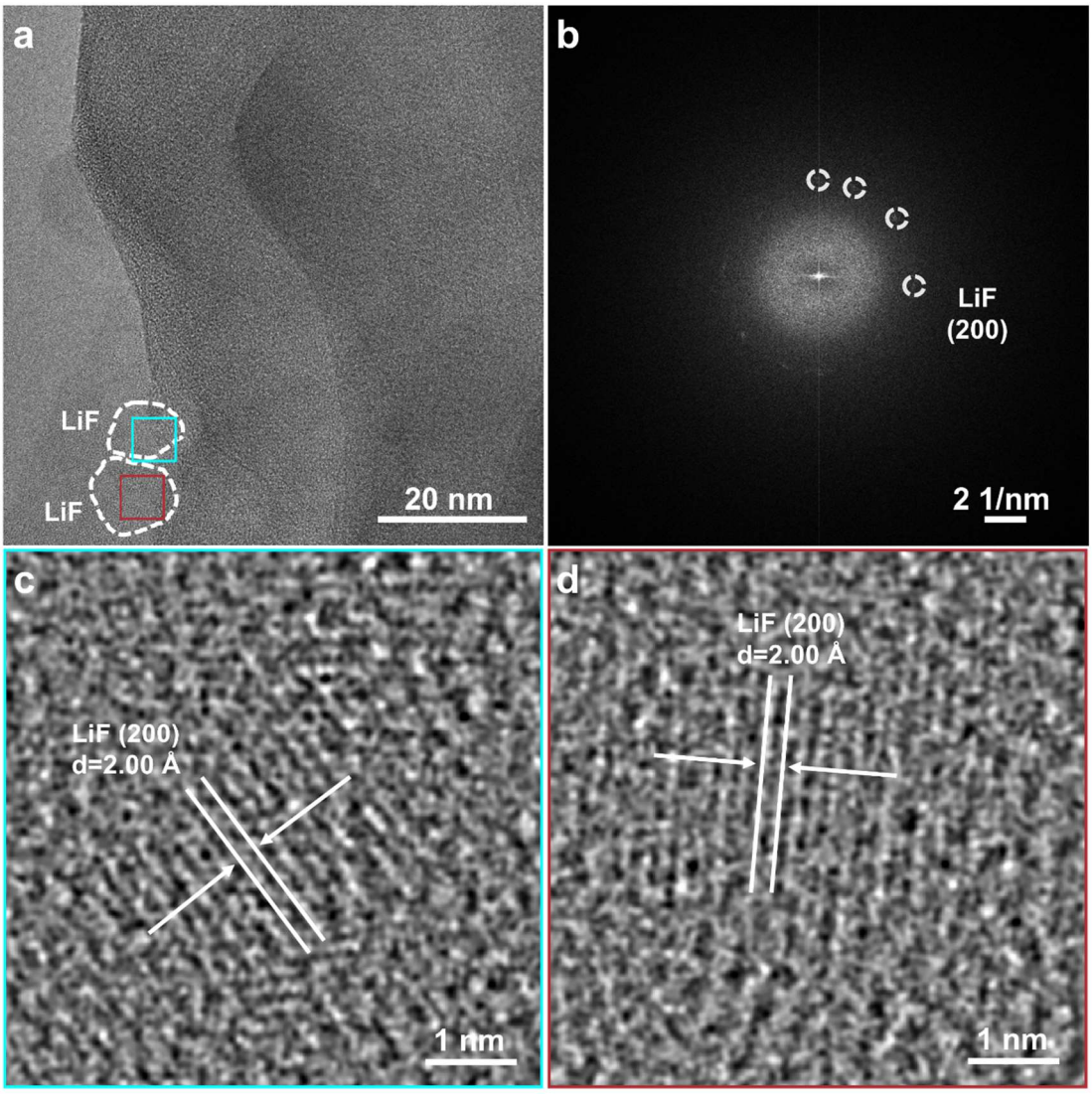

Fig. S10 (a) HRTEM image of Fig. 4d, (b) corresponding fast Fourier transformed images of the Si particle after 300 cycles and (c, d) corresponding magnified images of selected areas in (a).

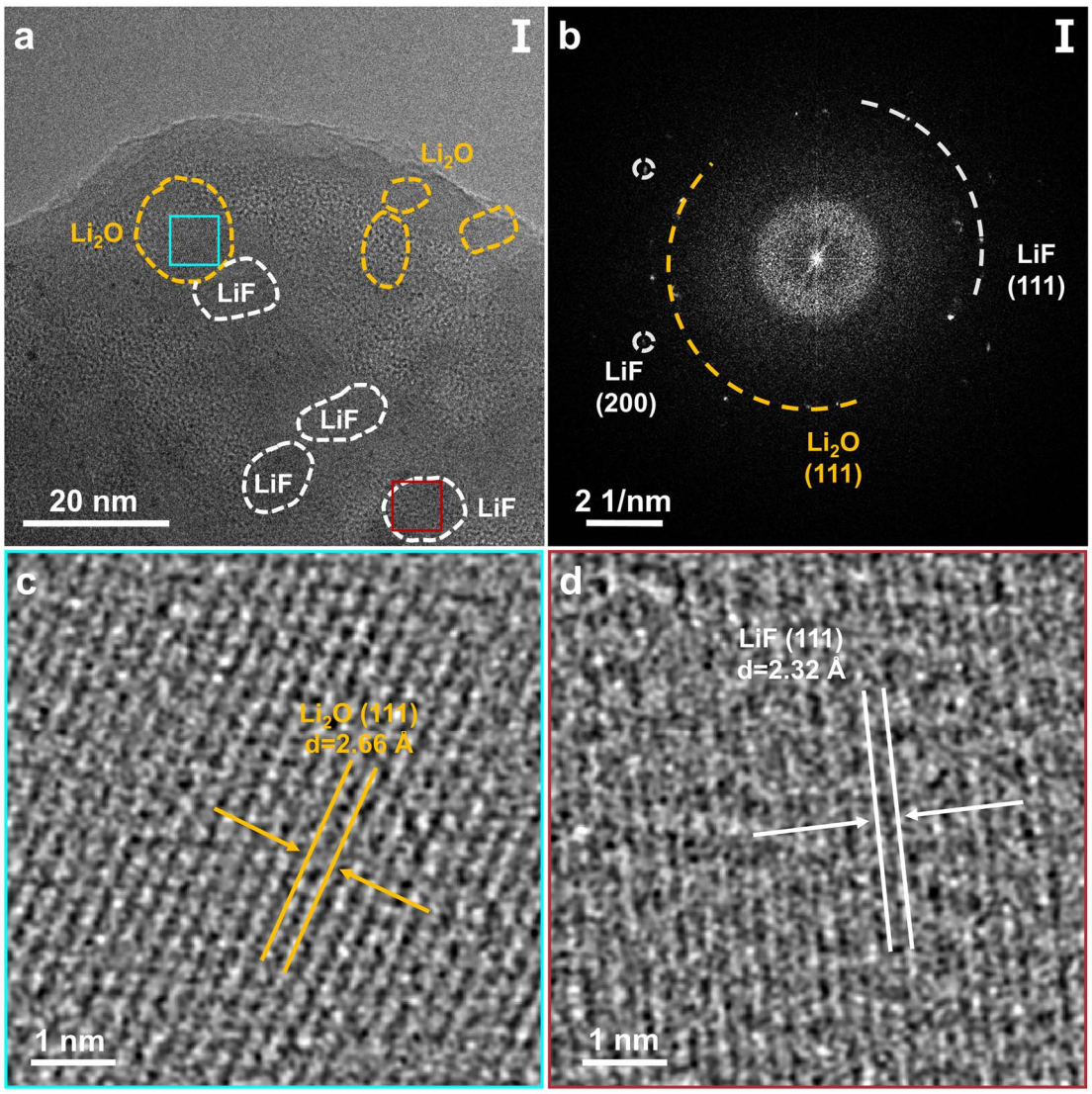

Fig. S11 (a) HRTEM image of area I in Fig. 5b, (b) corresponding fast Fourier transformed image and (c, d) corresponding magnified images of selected areas in (a).

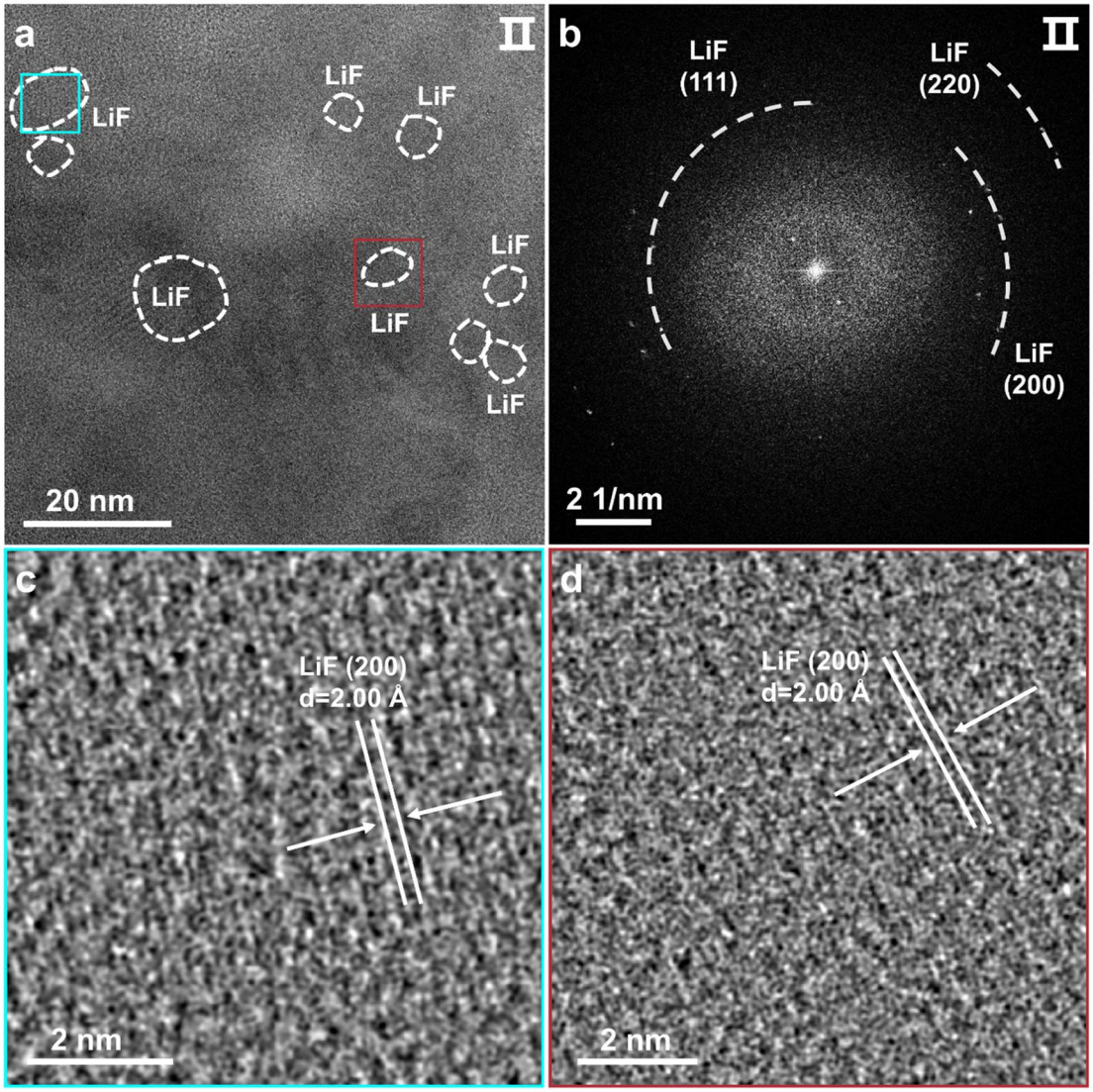

Fig. S12 (a) HRTEM image of area II in Fig. 5b, (b) corresponding fast Fourier transformed image and (c, d) corresponding magnified images of selected areas in (a).

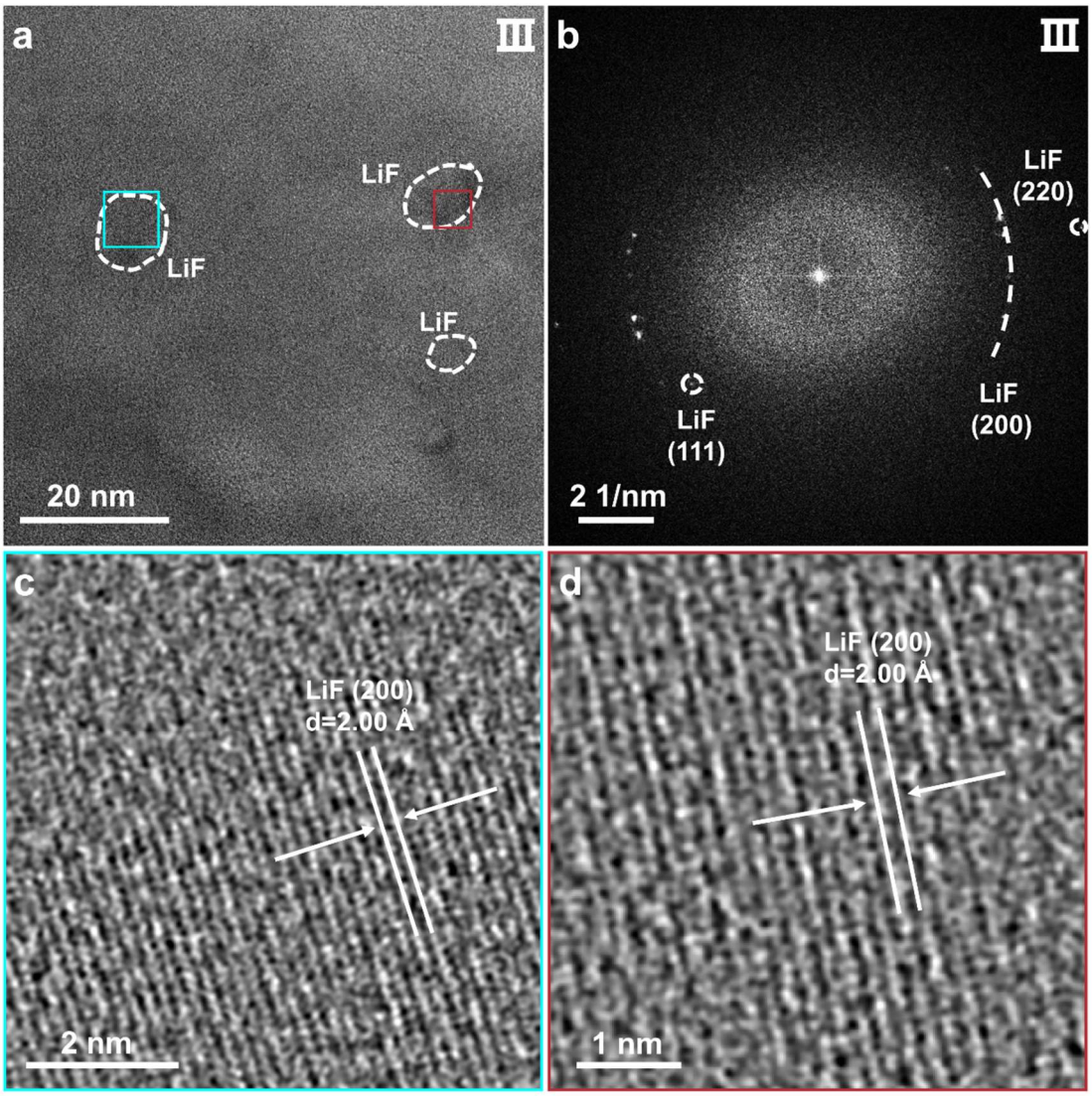

Fig. S13 (a) HRTEM image of area III in Fig. 5b, (b) corresponding fast Fourier transformed image and (c, d) corresponding magnified images of selected areas in (a).

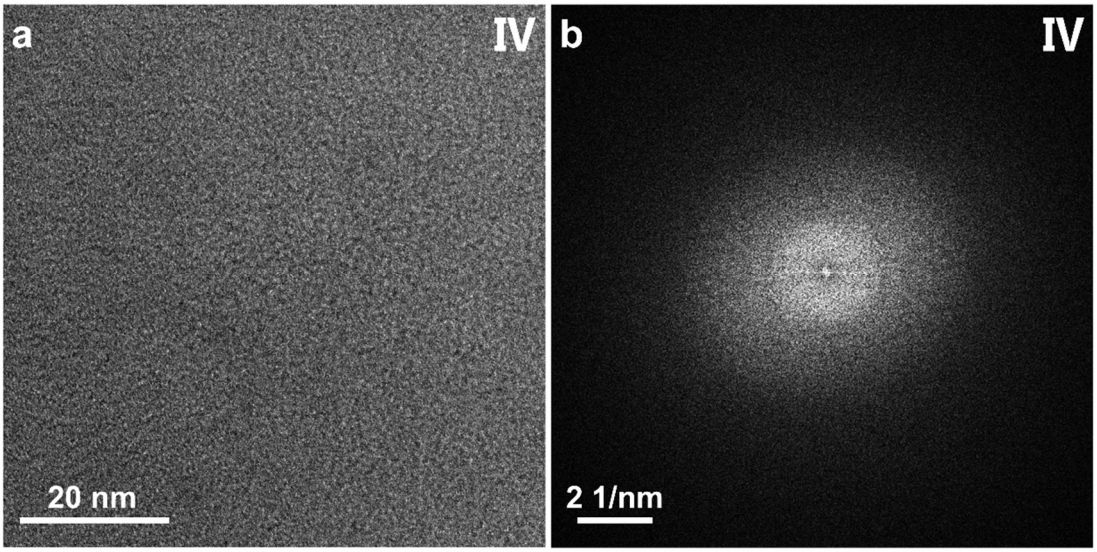

Fig. S14 (a) HRTEM image of area IV in Fig. 5b and (b) corresponding fast Fourier transformed image.

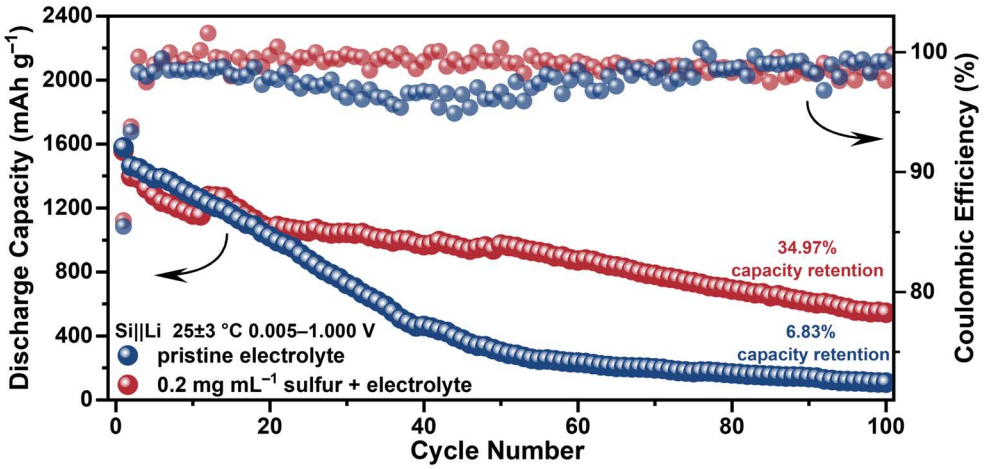

Fig. S15 Cycling performance of Si||Li coin cells with pristine electrolyte and sulfur-added (0.2 mg mL^{-1}) electrolyte.

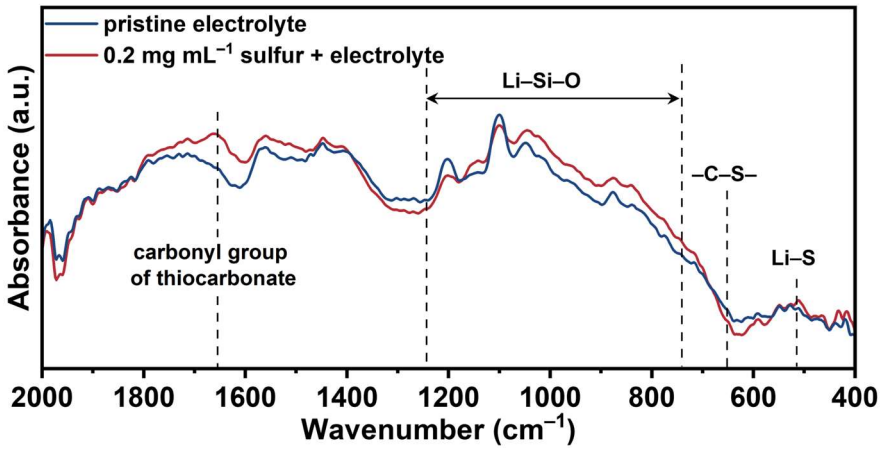

Fig. S16 FTIR-ATR spectra of Si electrodes after one cycle in Si||Li coin cells with pristine electrolyte and sulfur-added (0.2 mg mL^{-1}) electrolyte. The emerging peaks at 1654 cm^{-1} and 641 cm^{-1} correspond to the carbonyl group of thiocarbonate and C–S bond[10] indicating to form crosslinking SEI.

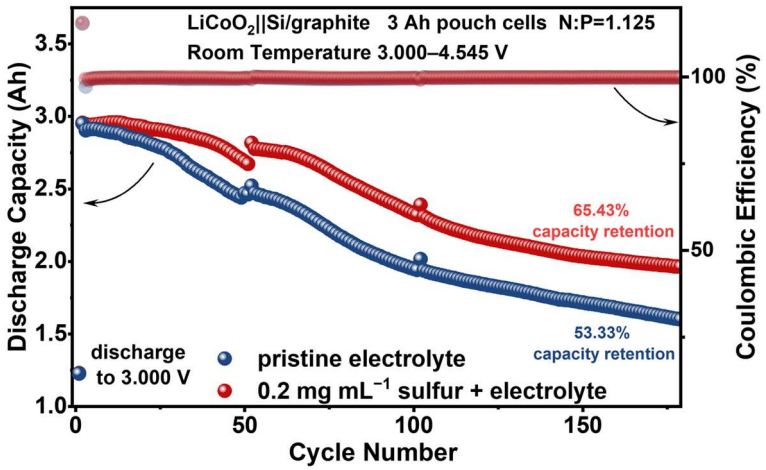

Fig. S17 Cycling performance of $LiCoO_2$||Si/graphite 3-Ah pouch cells with pristine electrolyte and sulfur-added (0.2 mg mL^{-1}) electrolyte.

Supplementary References

1. T. Subburaj, W. Brevet, F. Farmakis, D. Tsiplakides, S. Balomenou, N. Strataki, C. Elmasides, B. Samaniego and M. Nestoridi, *Electrochim. Acta*, 2020, **354**, 136652.
2. L. Hu, X. Zhang, P. Zhao, H. Fan, Z. Zhang, J. Deng, G. Ungar and J. Song, *Adv. Mater.*, 2021, **33**, 2104416.
3. L. Zhao, Y.-B. He, C. Li, K. Jiang, P. Wang, J. Ma, H. Xia, F. Chen, Y. He, Z. Chen, C. You and F. Kang, *J. Mater. Chem. A*, 2019, **7**, 24356-24365.
4. Q. Li, R. Yi, Y. Xu, X. Cao, C. Wang, W. Xu and J.-G. Zhang, *J. Power Sources*, 2022, **548**, 232063.
5. N. Yang, J. Sun, R. Shao, Z. Cao, Z. Zhang, M. Dou, J. Niu and F. Wang, *Cell Rep. Phys. Sci.*, 2022, **3**, 100862.
6. H. Wang, A. Shao, R. Pan, W. Tian, Q. Jia, M. Zhang, M. Bai, Z. Wang, F. Liu, T. Liu, X. Tang, S. Li and Y. Ma, *ACS Nano*, 2023, **17**, 21850-21864.
7. W. Zhang, S. Gui, Z. Zhang, W. Li, X. Wang, J. Wei, S. Tu, L. Zhong, W. Yang, H. Ye, Y. Sun, X. Peng, J. Huang and H. Yang, *Small*, 2023, **19**, 2303864.
8. Q. Ma, Z. Zhao, Y. Zhao, H. Xie, P. Xing, D. Wang and H. Yin, *Energy Storage Mater.*, 2021, **34**, 768-777.
9. W. An, B. Gao, S. Mei, B. Xiang, J. Fu, L. Wang, Q. Zhang, P. K. Chu and K. Huo, *Nat. Commun.*, 2019, **10**, 1447.
10. L. Yang, Y. Huang, M. K. Tufail, X. Wang and W. Yang, *Small*, 2022, **18**, 2202060.